

All-optical four-state magnetization reversal in (Ga,Mn)As ferromagnetic semiconductors

M. D. Kapetanakis¹, P. C. Lingos¹, C. Piermarocchi², J. Wang³, and I. E. Perakis¹

¹*Department of Physics, University of Crete and Institute of Electronic Structure & Laser, Foundation for Research and Technology-Hellas, Heraklion, Crete, 71110, Greece*

²*Department of Physics & Astronomy, Michigan State University, East Lansing, MI, 48824, USA and*

³*Ames Laboratory and Department of Physics and Astronomy, Iowa State University, Ames, Iowa 50011, USA*

(Dated: November 9, 2018)

Using density matrix equations of motion and a tight-binding band calculation, we predict all-optical switching between four metastable magnetic states of (III,Mn)As ferromagnets. This switching is initiated non-thermally within 100fs, during nonlinear coherent photoexcitation. For a single optical pulse, magnetization reversal is completed after ~ 100 ps and controlled by the coherent femtosecond photoexcitation. Our predicted switching comes from magnetic nonlinearities triggered by a femtosecond magnetization tilt that is sensitive to un-adiabatic light-induced spin interactions.

PACS numbers: 78.47.J-, 78.20.Ls, 42.65.Re

The goal of THz magnetic switches underlies the entire field of spin-electronics and challenges our understanding of fundamental non-equilibrium spin processes. The reading and writing of bits rely on reversing the magnetization direction between “up” and “down”. In conventional switching, the magnetization moves out of equilibrium via laser heating. A magnetic field then exerts a torque that reverses the magnetization within femtoseconds [1, 2]. This speed can be improved by using coherent spin rotation, via precession of the entire memory cell around a magnetic field pulse—precessional/ballistic switching [1–4]. This pulsed field must have duration of at least half the precession period (100’s of ps), which sets a fundamental limit of the magnetization reversal time. This speed is further limited by randomness [4] or weak precession damping allowing back-switching of magnetic elements (“ringing”) [2, 3]. Faster switching, within 100fs, could be explored by using laser pulses to inject spin-polarized carriers [5]. This is important for meeting the demand for improved read/write speeds, bit density, and reliability of current magnetic devices.

Magnetic properties of (III,Mn)V ferromagnetic semiconductors exhibit sensitive response to carrier density tuning via light, electrical gates, or spin currents. This holds promise for high-speed magnetic switches that combine information processing and storage on a single chip device with low power consumption [6]. The femtosecond photoexcitation of GaMnAs revealed distinct transient magneto-optical responses: (i) ultrafast decrease of the magnetization *amplitude* [7] within ~ 100 fs (demagnetization) [8–10], (ii) enhancement of magnetic order on ps timescale [11], (iii) magnetization re-orientation within ~ 100 fs, followed by a distinct ps regime of coherent precession [12, 13]. Such non-equilibrium magnetic effects appear to be universal [7, 14, 15]. The pioneering work of Bigot and collaborators [7], who observed demagnetization on a ~ 100 fs timescale much shorter than the spin-phonon relaxation time, thus evolved into a new

field of *femto-magnetism*. However, the many-body theory of femto-magnetism remains controversial [5, 15] and must ultimately engage the elements of transient coherence, correlation, and nonlinearity *on an equal footing*. Here we present such a mean field theory and propose a nonthermal mechanism for achieving ultrafast all-optical magnetization switching in ferromagnetic (Ga,Mn)As.

We use a *single* 100fs optical pulse at ~ 3 eV, in resonance with the strong peak in the density of states for $\Lambda_3 \rightarrow \Lambda_1$ interband transitions along the eight equivalent $\{111\}$ directions of the GaAs Brillouin zone (the Λ -edge) [16]. Magnetization switching is initiated within ~ 100 fs via *non-thermal* spin manipulation. To describe this, we consider the Hamiltonian $H(t) = H_b + H_{exch}(t) + H_L(t)$, where $H_b = H_0 + H_{SO} + H_{pd}$ is the standard Hamiltonian describing *un-excited* (Ga,Mn)As bands [6, 17]. H_0 describes the states in the presence of the lattice potential, while H_{SO} is the spin-orbit interaction [17]. We consider hole densities $\sim 10^{20} \text{cm}^{-3}$ where the virtual crystal approximation applies [6]. H_{pd} is the mean-field interaction [6, 18] of the hole spin with the *ground state* Mn spin \mathbf{S}_0 , whose strength $\beta = 24 \text{ meV nm}^3$ was extracted from experiment [12]. H_{pd} lifts the degeneracy of the GaAs bands [17] by the magnetic exchange energy $\Delta_{pd} = 88 \text{ meV}$. Below we describe microscopically a photo-induced magnetic anisotropy characterized by the energy ratio E_{SO}/Δ_{pd} ($E_{SO} \sim 350 \text{ meV}$ is the spin-orbit energy), which is *not* due to thermal [14] effects. For this we start by diagonalizing H_b using the Slater-Koster sp^3s^* tight-binding Hamiltonian [17]. We thus obtain a basis of valence hole (conduction electron) states created by $\hat{h}_{\mathbf{k}n}^\dagger$ ($\hat{e}_{\mathbf{k}n}^\dagger$), where \mathbf{k} is the crystal momentum and n labels the 20 bands [17]. This static bandstructure is modified by the interaction $H_{exch}(t)$ of the hole spin with the photoexcited deviation $\Delta\mathbf{S}(t)$ of the collective Mn spin \mathbf{S} from \mathbf{S}_0 [13, 18]. Here we treat $H_{exch}(t)$ at the Hartree-Fock level, which conserves the magnetization amplitude, and note that demagnetization [10] arises

from correlations considered in Ref. [19]. $H_L(t)$ describes the interband dipole coupling of the optical field $\mathbf{E}(t)$, which propagates along [001] and is linearly polarized at an angle of $\sim 2^\circ$ from [100]. H_L leads to nonlinear couplings between the bands, characterized by the Rabi energies $d_{nm\mathbf{k}}(t) = d_{nm\mathbf{k}} \exp[-i\omega_p t - t^2/\tau_p^2]$, where $\omega_p = 3\text{eV}$, $\tau_p = 100\text{fs}$, and $d_{nm\mathbf{k}} = \mu_{nm\mathbf{k}} \mathbf{E}$. The matrix elements $\mu_{nm\mathbf{k}}$ were obtained from the tight-binding parameters of H_b as in Ref.[20]. We derived coupled density matrix equations of motion for \mathbf{S} , all nonthermal populations, and the photoinduced transient coherences between *all* conduction and valence bands [13, 18]. The dynamics of these coherences, neglected within the semiclassical rate equation treatment of spin photoexcitation, is important for determining the photoexcited hole spin $\mathbf{s}_h(t)$. For details, see Refs. [13, 17, 18, 20] and a future publication.

The Mn spin is obtained from the equation of motion

$$\partial_t \mathbf{S} = -\beta \mathbf{S} \times \mathbf{s}_h - \gamma \mathbf{S} \times \mathbf{H}_{\text{th}} + \frac{\alpha}{S} \mathbf{S} \times \partial_t \mathbf{S}, \quad (1)$$

where γ is the gyromagnetic ratio and α the Gilbert damping coefficient [21]. Our mean-field approximation misses demagnetization [10], which can be included phenomenologically [14] or microscopically [19]. Here, the photoexcited hole spin creates an effective magnetic field pulse, $\gamma \mathbf{H}_{ph}(t) = \beta \mathbf{s}_h(t)$, which transiently modifies the magnetic anisotropy and triggers nonthermal switching. \mathbf{s}_h is obtained microscopically after noting that

$$\mathbf{s}_h = \frac{1}{V} \sum_{n\mathbf{k}} \mathbf{s}_{\mathbf{k}n}^h \langle \hat{h}_{\mathbf{k}n}^\dagger \hat{h}_{\mathbf{k}n} \rangle + \frac{1}{V} \sum_{n \neq n' \mathbf{k}} \mathbf{s}_{\mathbf{k}n}^h \langle \hat{h}_{\mathbf{k}n}^\dagger \hat{h}_{\mathbf{k}n'} \rangle, \quad (2)$$

where V is the volume. $\mathbf{s}_{\mathbf{k}n}^h$ are the hole spin matrix elements with respect to the eigenstates of H_b . They describe spin mixing due to H_{SO} and H_{pd} . The first term in Eq.(2) is roughly proportional to the photoexcited hole density. For $\omega_p = 3\text{eV}$, it comes from the transient population of high energy states close to the Λ point; these do not contribute to the ground state magnetic anisotropy. The second term in Eq.(2) comes from the coherences $\langle \hat{h}_{\mathbf{k}n}^\dagger \hat{h}_{\mathbf{k}n'} \rangle$, $n \neq n'$, photoinduced via Raman processes. Here we solved the nonlinear equations of motion that give all $\langle \hat{h}_{\mathbf{k}n}^\dagger \hat{h}_{\mathbf{k}m} \rangle$ at the eight \mathbf{k} 's with maximum density of states (Λ -point). The mean field arising from all \mathbf{k} will be considered elsewhere. The dynamics depends on $H_{exch}(t)$ and the nonlinear polarizations $\langle \hat{h}_{-\mathbf{k}n} \hat{e}_{\mathbf{k}m} \rangle$, obtained from their equations of motion [13, 18]. We thus describe the effect on $\mathbf{s}_h(t)$ of (i) static bandstructure and the competition of spin-orbit and magnetic exchange interactions, (ii) photoinduced interactions that transiently change the bandstructure, and (iii) nonlinear coherence. We considered dephasing/relaxation times $\sim 30\text{fs}$ [6].

The Γ -point *thermal* hole Fermi sea [6] is clearly distinguished from the carriers that create $\mathbf{s}_h(t)$, which are photoexcited at $\sim 3\text{eV}$. Our main assumption is that, within time intervals $\sim 100\text{fs}$, the Fermi sea adjusts adi-

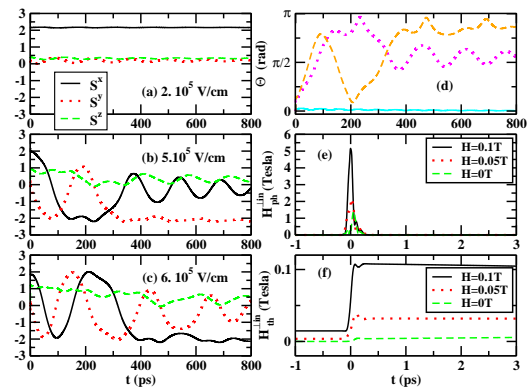


FIG. 1: (color online) (a)–(c): $\mathbf{S}(t)$ for $H=100\text{mT}$, $\alpha=0.03$ [21], and three pump fluences. $K_c=0.0144\text{meV}$, $K_u=0.0025\text{meV}$, and $K_{uz}=5K_c$ give anisotropy fields 1.7mT, 0.29mT, and 8.3 mT [6]. (d): Angle $\cos \Theta = \hat{\mathbf{S}}_0 \cdot \hat{\mathbf{S}}(t)$, $0 \leq \Theta(t) \leq \pi$. (e): In-plane component of the non-thermal field $\gamma \mathbf{H}_{ph}^\perp = \beta (\mathbf{s}_h)^\perp$. (f): Thermal field component \mathbf{H}_{th}^\perp .

abatically to the transient changes in the Mn spin order parameter and can thus be described in terms of its total energy $E_h[\mathbf{S}(t)]$. E_h then depends on the instantaneous Mn spin (unit vector $\hat{\mathbf{S}}$) and the second term in Eq.(1) describes precession around the *thermal* magnetic anisotropy field $\gamma \mathbf{H}_{th} = -\partial E_h / \partial \mathbf{S}$ [5, 14]. Symmetry [22, 23] dictates that, independent of issues surrounding the bands close to the bandgap of (Ga,Mn)As [6, 10],

$$E_h = K_c (\hat{S}_x^2 \hat{S}_y^2 + \hat{S}_x^2 \hat{S}_z^2 + \hat{S}_y^2 \hat{S}_z^2) + K_{uz} \hat{S}_z^2 - K_u \hat{S}_x \hat{S}_y - \gamma H S_z \quad (3)$$

as observed experimentally [23]. K_c is the cubic anisotropy constant, K_{uz} is the uniaxial constant due to strain and shape anisotropies, K_u describes an in-plane anisotropy that may be due to materials issues [23], and H is an external magnetic field along [001]. We extract these parameters from experiment [23] and neglect any transient temperature effects, which enhance our predicted anisotropy and give demagnetization [10, 14]. We thus obtain a *biaxial* magnetic anisotropy with *four* metastable magnetic ground states [12, 24]. Since the easy axes are close to $y=0$ or $x=0$, we label these four magnetic ground states by X^\pm and Y^\pm [12].

Figures 1(a), (b) and (c) show $\mathbf{S}(t)$ for initial condition along X^+ and three pump fluences. They clearly demonstrate magnetic switching controlled nonthermally by the pump pulse. Fig. 1(a) was obtained for $E=2 \times 10^5 \text{V/cm}$, as in the experiment of Ref.[12] (fluence $\sim 7 \mu\text{J/cm}^2$). In this case, $\Delta \mathbf{S}$ is small and \mathbf{s}_h excites magnon oscillations. These results agree with Ref.[12]. With increasing pump intensity, the magnetic nonlinearities of Eq. (3) kick in. For $E=5 \times 10^5 \text{V/cm}$, we obtain $X \rightarrow Y$ switching after $\sim 400\text{ps}$ (to Y^-), while for intermediate times, the magnetization reverses direction (to X^- , Fig.1 (b)). For $E=6 \times 10^5 \text{V/cm}$, the magnetization reversal is com-

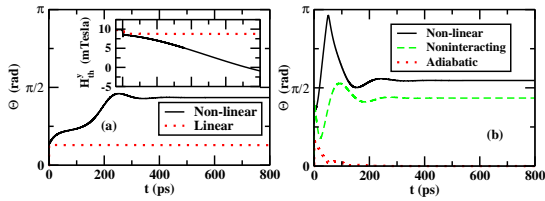


FIG. 2: (color online) Nonlinear magnetization dynamics ($\alpha=0.3$, $E=6\times 10^5$ V/cm). (a): Comparison of Mn spin re-orientation angles $\Theta(t)$ and thermal anisotropy field H_{th}^y along [010] (inset) during ~ 100 ps and ~ 10 ps timescales. (b): Comparison of full calculation (solid line) with result obtained by neglecting $H_{exch}(t)$ (dashed line) and within semiclassical adiabatic approximation of spin photoexcitation (dotted line).

plete after ~ 400 ps (to X^- , Fig.1 (c)). Fig.1(d) shows this switching more clearly, by plotting the magnetization reorientation angle $\Theta(t) = \cos^{-1}(\hat{\mathbf{S}}_0 \cdot \hat{\mathbf{S}})$ ($0 \leq \Theta \leq \pi$). Our scheme could thus potentially be used to write multiple bits in a massively parallel memory with THz speed, since one normally reads bits long after writing them.

Our switching is initiated by the photoinduced nonthermal (\mathbf{H}_{ph}) field (Fig.1(e)) and completed by the thermal (\mathbf{H}_{th}) field (Fig. 1(f)). \mathbf{H}_{ph} only lasts for ~ 100 fs and is enhanced by the external magnetic field H . For given intensity, \mathbf{H}_{ph} is much stronger for $\omega_p=3$ eV than for $\omega_p=1.5$ eV due to the difference in the density of states and spin-orbit interaction [13]. In contrast, the thermal field \mathbf{H}_{th} develops as E_h changes due to the Mn spin $\Delta\mathbf{S}(t)$ photoinduced by s_h . It is much weaker than \mathbf{H}_{ph} during the first 100's of fs but dominates over ~ 100 ps.

We now turn to the origin of the photo-induced nonlinear behavior demonstrated by Fig.1. By expanding \mathbf{H}_{th} to first order in $\Delta\mathbf{S}$, we obtain the linear spin dynamics shown by the dotted lines in Fig.2 (a). The difference between the linear and nonlinear Mn spin re-orientation angle $\Theta(t)$ is small during fs timescales but grows over many ps. To interpret this, the inset of Fig. 2 shows that H_{th}^y , the component perpendicular to \mathbf{S}_0 , grows over 10's of ps due to the cubic anisotropy nonlinearity $\propto S_y^3$, as S_y increases due to precession around H_{th}^z . In turn, S_z (and thus H_{th}^z) increases due to precession around H_{th}^y . Switching is triggered by this nonlinear dependence, as \mathbf{H}_{th} builds over 10's of ps until the magnetization overcomes the energy barrier between the magnetic states.

Fig.2(b) shows that the time-dependent changes in the bandstructure H_b , due to the photoinduced interaction $H_{exch}(t)$, affect s_h and $\Theta(t)$ (compare solid and dashed lines). The dotted line in Fig.2(b) also shows that the semiclassical Fermi's Golden rule hole spin generation rate, obtained by solving our equations within the adiabatic approximation while treating the interactions perturbatively [25], can also give strong deviations. We conclude that our treatment of the coherent nonlinear photoexcitation of the interacting system is important

for modelling the magnetization dynamics.

In summary, we predict spin switchings triggered by coherent nonlinear photoexcitation of (III,Mn)V ferromagnets by a *single* femtosecond optical pulse. We obtained all-optical magnetization reversal and demonstrated a four-state magnetic switching functionality resulting from the interplay between ultrafast coherence, nonlinearity, and competing spin interactions. Our proposed effect should be confirmed experimentally with femtosecond magneto-optical spectroscopy and points to future possibilities for further reducing the switching times by using multiple coherent optical pulses.

This work was supported by the EU ITN program ICARUS, the U.S. National Science Foundation grant DMR-1055352, and the U.S. Department of Energy-Basic Energy Sciences under contract DE-AC02-7CH11358.

-
- [1] J. Stöhr and H. C. Siegmann, *Magnetism: From Fundamentals to Nanoscale Dynamics* (Springer, Berlin, 2006).
 - [2] H. W. Schumacher *et al.*, Phys. Rev. Lett. **90**, 017204 (2003).
 - [3] Th. Gerrits *et al.*, Nature **418**, 509, (2002).
 - [4] I. Tudosa *et al.*, Nature **428**, 831 (2004).
 - [5] A. Kirilyuk, A. V. Kimel, and T. Rasing, Rev. Mod. Phys. **82**, 2731 (2010).
 - [6] T. Jungwirth *et al.*, Rev. Mod. Phys. **78**, 809 (2006).
 - [7] E. Beaurepaire *et al.*, Phys. Rev. Lett. **76**, 4250 (1996); L. Guidoni *et al.*, Phys. Rev. Lett. **89**, 17401 (2002).
 - [8] J. Wang *et al.*, J. Condes. Matter **18** R501 (2006).
 - [9] J. Wang *et al.*, Phys. Rev. Lett. **95**, 167401 (2005); J. Wang *et al.*, Phys. Rev. B **77**, 235308 (2008)
 - [10] L. Cywiński and L. J. Sham, Phys. Rev. B **76**, 045205 (2007); O. Morandi, P.-A. Hervieux, and G. Manfredi, Eur. Phys. J. D **52**, 155 (2009).
 - [11] J. Wang *et al.*, Phys. Rev. Lett. **98**, 217401 (2007).
 - [12] J. Wang *et al.*, Appl. Phys. Lett. **94**, 021101 (2009).
 - [13] M. D. Kapetanakis *et al.*, Phys. Rev. Lett. **103**, 047404 (2009).
 - [14] J.-Y. Bigot *et al.*, Chem. Phys. **318**, 137 (2005).
 - [15] J.-Y. Bigot *et al.*, Nature Phys. **5**, 515 (2009); C. Boeglin *et al.*, Nature **465**, 458 (2010).
 - [16] K. S. Burch *et al.*, Phys. Rev. B **70**, 205208 (2004).
 - [17] P. Vogl *et al.*, J. Phys. Chem. Solids **44**, 365 (1983).
 - [18] J. Chovan, E. G. Kavousanaki, and I. E. Perakis, Phys. Rev. Lett. **96**, 057402 (2006); J. Chovan and I. E. Perakis, Phys. Rev. B **77**, 085321 (2008).
 - [19] M. D. Kapetanakis and I. E. Perakis, Phys. Rev. Lett. **101**, 097201 (2008); Phys. Rev. B **78**, 155110 (2008).
 - [20] L. C. Lew Yan Voon and L. R. Ram-Mohan, Phys. Rev. B **47**, 15500 (1993).
 - [21] D. M. Wang *et al.*, Phys. Rev. B **75**, 233308 (2007); J. Qi *et al.*, Phys. Rev. B **79**, 085304 (2009).
 - [22] M. Abolfath *et al.*, Phys. Rev. B **63**, 054418 (2001); T. Dietl, *et al.*, Phys. Rev. B **63**, 195205 (2001).
 - [23] U. Welp *et al.*, Phys. Rev. Lett. **90**, 167206 (2003)
 - [24] G. V. Astakhov *et al.*, Appl. Phys. Lett. **86**, 152506 (2005).
 - [25] F. Rossi and T. Kuhn, Rev. Mod. Phys. **74**, 895 (2002).